Journal Applied Mechanics and Technical Physics, Vol. 37, No. 1, 1996

RAREFACTION SHOCK WAVE IN A POROUS MATERIAL

S. P. Kiselev and V. M. Fomin

UDC 539.374

Let us consider an elastoplastic material containing a large number N of spherical pores. An exact solution of the problem of deformation of such a material is practically impossible. Therefore, an approximate approach is in wide spread use in which averaging methods are used to reduce an N-connected continuum to a porous body with certain effective characteristics. A large number of averaging methods exist currently and is surveyed in [1]. The present paper deals with averaging a cell. The technique of averaging on a porous elastoplastic material was developed in [2–8], where it was assumed that plastic deformations in a porous body start when mean stresses reach the yield surface. For a porous material this condition is insufficient. In particular, if the average pressure is rather high, then under the effect of pressure there appears a plastic region near the pore and plastic deformations occur even when mean stresses do not lie on the yield surface. A mathematical model accounting for the effect of the plastic zone on deformation of a plastic material was constructed in [9, 10]. Numerical calculations in [11] have shown that the model describes well the propagation of shock waves (SW) in porous iron [12]. On the basis of the model, we study the propagation of rarefaction shock waves (RSW) in porous iron.

Following [9–11], we write the equations of deformation of a porous material in the one-dimensional nonsteady case:

$$\frac{\partial\rho}{\partial t}+\rho\frac{\partial v}{\partial x}=0,\quad \rho=\rho_s m_2,\quad m_1+m_2=1,\quad \rho\frac{\partial v}{\partial t}-\frac{\partial\sigma_1}{\partial x}=0,\quad \frac{\partial x}{\partial t}=v,\quad \sigma_1=S_1-p,$$

$$\rho\frac{\partial\mathcal{E}}{\partial t}-\sigma_1\frac{\partial\varepsilon_1}{\partial t}=0,\quad \varepsilon_1=\frac{\partial u}{\partial x},\quad \dot\varepsilon_1=\frac{\partial v}{\partial x},\quad u=x-x_0,\quad \dot p=\dot p_{\mathrm x}+\dot p_T,\quad \dot p_{\mathrm x}=-K\dot\varepsilon_{kk},\quad \dot p_T=(\Gamma\rho\mathcal{E}_T)^{\cdot},$$

$$\mathcal{E}=\mathcal{E}_{\mathrm x}+\mathcal{E}_T,\quad \mathcal{E}_{\mathrm x}=\frac{1}{2\rho}\left(K_1(\varepsilon^e_{kk})^2+3\mu_1(e^e_1)^2\right),\quad \varepsilon_i=e_i+\frac{1}{3}\,\varepsilon_{kk},\quad \varepsilon_{kk}=\varepsilon_1,\quad \dot\varepsilon_{kk}=\dot\varepsilon^e_{kk}+\dot\varepsilon^p_{kk},$$

$$\dot e_i=\dot e^e_i+\dot e^p_i,\quad i=1,2,3,\quad \dot S'_i=(2\mu e_i)^{\cdot},\quad S_i=\begin{cases} S'_i, & \dfrac{3}{2}\displaystyle\sum_{i=1}^{3}(S'_i)^2<Y^2,\\ \sqrt{\dfrac{2}{3}}S'_iY\Big/\sqrt{\displaystyle\sum_{i=1}^{3}(S'_i)^2}; \end{cases}\tag{1}$$

when $|p|<|p_0|$

$$K=K_1,\quad \mu=\mu_1,\quad \frac{\Gamma}{\Gamma_s}=\frac{K}{K_sm_2},\quad |p_0|=\frac{2}{3}\,Y_s\overline{m}_2,\quad \overline{m}_1=qm_1,\quad \overline{m}_1+\overline{m}_2=1,$$

$$q=1.7,\quad Y^2=Y_s^2\overline{m}_2^2-\frac{9}{4}\,p^2\overline{m}_1,\quad K_1=\frac{K_sm_2}{1+\dfrac{m_1}{2}\left(\dfrac{1+\nu}{1-2\nu}\right)},\quad \mu_1=\frac{\mu_sm_2}{1+0.5m_1};\tag{2}$$

when $|p_0|\leqslant|p|<|p_*|$

$$K=K_2,\quad \mu=\mu_2,\quad \frac{\Gamma}{\Gamma_s}=\frac{K}{K_sm_2},\quad |p_*|=\frac{2}{3}\ln\left(\frac{1}{\overline{m}_1}\right),\quad Y^2=Y_s^2\overline{m}_2m_e^2,\quad m_e+m_p=1,$$

Institute of Theoretical and Applied Mechanics, Siberian Division, Russian Academy of Sciences, Novosibirsk 630090. Translated from Prikladnaya Mekhanika i Tekhnicheskaya Fizika, Vol. 37, No. 1, pp. 28–35, January–February, 1996. Original article submitted February 24, 1995.

0021-8944/96/3701-0023 $15.00

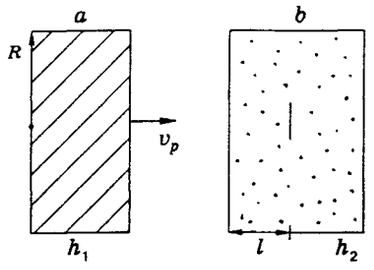

Fig. 1

$$K_2 = \frac{K_s m_2}{1 + \dfrac{(1+\nu)Y_s}{3(1-2\nu)|p|} m_p m_2}, \quad \mu_2 = \frac{\mu_s m_e}{\dfrac{m_e}{m_p} + 0.5 m_p}, \quad e_i^e = \frac{S_i}{2\mu_1}, \quad \dot{\varepsilon}_{kk}^e = -\frac{K_2 \dot{\varepsilon}_{kk}}{K_1} + \frac{\dot{m}_2}{m_2},$$

$$\frac{3\chi p}{2Y_s} + 1 - m_p + \ln\left(\frac{m_p}{\overline{m}_1}\right) = 0, \quad |p_0| \leqslant |p| < |p_+|,$$

$$m_e = \frac{\xi}{1+\xi} + \frac{3\chi(p - p_+)}{\xi Y_s}, \quad |p_+| < |p| < |p_z|, \tag{3}$$

$$p_+ = \frac{2}{3}\chi Y_s\left(\ln\left(\frac{1}{\overline{m}_1}\right) + \frac{\xi}{1+\xi} + \ln\left(\frac{1}{1+\xi}\right)\right), \quad \xi = \sqrt{\overline{m}_2},$$

$$p_z = p_+ - \frac{2\chi Y_s \overline{m}_2}{3(1+\xi)}, \quad \chi = \begin{cases} 1, & p < 0, \\ -1, & p > 0; \end{cases}$$

when $|p| \geqslant |p_*|$

$$\frac{2}{3}\chi Y_s \ln\left(\frac{1}{\overline{m}_1}\right) - \frac{4\eta \dot{m}_1}{3m_1} - p = 0, \quad \dot{p}_x = -K_1 \dot{\varepsilon}_{kk}^e, \quad \dot{\varepsilon}_{kk}^e = \frac{\dot{m}_2}{m_2} - \frac{\dot{\rho}}{\rho}, \quad \dot{e}_i^e = \frac{\dot{S}_i}{2\mu_1}. \tag{4}$$

Here ρ_s, ρ, p, S_i, $\mathcal{E}$, $\mathcal{E}_x$, $\mathcal{E}_T$, p_x, p_T, ε_1, $\dot{\varepsilon}_1$, u, v, σ_1, m_1, m_e, and m_p are the density of the material, the average density, the pressure, the stress deviator, the specific internal, cold, and thermal energies, the cold and thermal pressures, the strain, the strain rate, the dislocation, the velocity, the stress, the porosity, and the volume fraction of the material in the elastic and plastic states; Γ, ν, K_s, μ_s, Y_s, K_i, μ_i, Y, and η are the Gruneisen coefficient and Poisson's ratio; the volume compression, shear moduli, and yield strength of the material; the averaged moduli of volume compression, shear, and yield strength; and the viscosity of the material. A dot denotes the complete time derivative. In the case $|p| > |p_0|$ a plastic zone appears in the vicinity of the pore, and deformations become elastoplastic and are described by Eqs. (3) and (4). These formulas are valid at the loading stage ($p\dot{p} > 0$). For the unloading stage ($p\dot{p} < 0$) one should use Eqs. (2).

Equations (1)–(4) were solved numerically using a finite-difference method with a cross-mesh pattern. To diffuse SW fronts an artificial viscosity was used, which was selected in the same way as in [13].

Let us consider a uniform iron plate (Fig. 1a) of thickness $h_1 = 4$ mm, which strikes, with velocity $v_p = 0.236$ mm/μsec, a porous iron plate (Fig. 1b) of thickness $h_2 = 17$ mm and porosity $m_1^0 = 10^{-2}$. The mechanical properties of iron (steel) are the same as in [11]:

$$\rho_s = 7.85 \text{ g/cm}^3, \quad \Gamma = 2, \quad \mu_s = 80 \text{ GPa}, \quad K_s = 160 \text{ GPa},$$

$$Y_s = (Y_0 + \eta \dot{\varepsilon}_1^p)(1 + b_s(\varepsilon_1^p)^m), \quad Y_0 = 0.4 \text{ GPa}, \quad b_s = 2, \quad m = 1/2.$$

In our case, the strain rate does not exceed 10^5 sec^{-1}; therefore, following [14], the viscosity of iron is $\eta = 3 \cdot 10^3$ Pa$\cdot$sec.

The stress profiles $\sigma_1(x)$ for several time moments with the time step $\Delta t = 0.5$ μsec are presented in Fig. 2 (broken line is the interface between porous and uniform iron). One can see that the compression wave decomposes into three waves, and the rarefaction wave transforms into an RSW to the moment $t = 2$ μsec. To

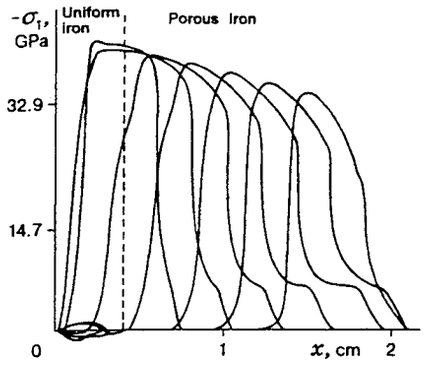

Fig. 2

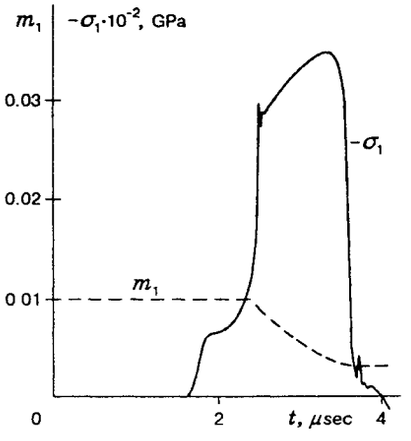

Fig. 3

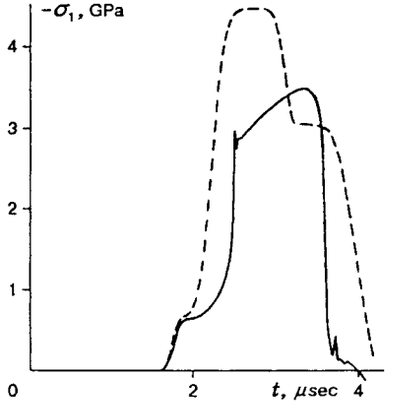

Fig. 4

calculate RSW we introduced an artificial viscosity. The dependences $\sigma_1(t)$ and $m_1(t)$ at the depth $l = 10$ mm are presented in Fig. 3. The dependence $\sigma_1(t)$ at $l = 10$ mm in porous and uniform iron is shown in Fig. 4 (solid and broken lines).

A SW in a porous body has a three-wave structure and consists of a spring forerunner, a "frozen" wave, and a relaxation zone. It is seen from Fig. 3 that the porosity in a "frozen" SW does not change. The pores are collapsed in the relaxation zone, which results in a pressure rise related to the change of porosity according to the equation

$$p = \frac{2}{3} Y_s \ln \frac{1}{m_1} - \frac{4}{3} \eta \frac{\dot{m}_1}{m_1}.$$

To explain RSW we find the propagation velocity of disturbances during unloading. The equation of motion is of the form

$$\rho \frac{dv}{dt} = \frac{\partial \sigma_1}{\partial x}, \qquad \sigma_1 = S_1 - p.$$

As follows from the calculations (see Fig. 3), the change of porosity in the rarefaction wave can be neglected, and therefore taking account of $dp \approx K_1 d\rho/\rho$ and $\partial\sigma_1/\partial x = (\partial S_1/\partial\rho - \partial p/\partial\rho)(\partial\rho/\partial x)$ we obtain

$$\frac{\partial \rho}{\partial t} + \rho \frac{\partial v}{\partial x} + v \frac{\partial \rho}{\partial x} = 0, \quad \frac{\partial v}{\partial t} + v \frac{\partial v}{\partial x} + \frac{a^2}{\rho} \frac{\partial \rho}{\partial x} = 0, \quad a^2 = -\frac{\partial S_1}{\partial \rho} + \frac{K_1}{\rho}$$

(a is the speed of sound). Hence it follows that the propagation velocity of disturbances is determined from

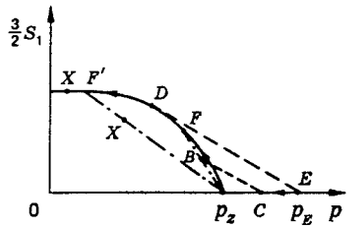

Fig. 5

the formula $dx/dt = v \pm a$. As mentioned before, since the stress $\sigma_1(E)$ behind the SW lies much higher than the critical pressure $|p_*|$, at point E we have $\sigma_1(E) = -p_E$, $Y = 0$ (Fig. 5, where the solid line shows the dependence $Y(p)$ and the point p_E corresponds to the pressure behind the SW). Rarefaction to pressure p_z occurs along the abscissa axis $S_1 = 0$, so $\partial S_1/\partial\rho = 0$, $a_- = \sqrt{K_1/\rho}$. After attaining the point p_z the speed of sound increases abruptly to $a_+ = \sqrt{K_1/\rho - \partial S_1/\partial\rho}$ $[\partial S_1/\partial\rho = (\partial S_1/\partial p)(K_1/\rho) < 0]$.

Depending on the gradient of the curve $Y(p)$ at the point $p_z - 0$ rarefaction can have either elastic (dot-and-dash line) or plastic character along the line $Y(p)$. To answer the question we find the increment of elastic stress $dS_1^e = 2\mu_1 de_1$ and the stress on the yield surface $dS_1^p = (2/3)dY$ during deformation $d\varepsilon_1 = -d\rho/\rho$. If $dS_1^e < dS_1^p$, the deformation is elastic, while with the reverse inequality, it is elastoplastic. Using the relations $de_1 = (2/3)\,d\varepsilon_1$, $dY = (\partial Y/\partial p)(dp/d\rho)d\rho$, and $dp/d\rho = K_1$, we have

$$dS_1^e = -\frac{4}{3}\mu_1\frac{d\rho}{\rho}, \qquad dS_1^p = -\frac{2}{3}\left|\frac{\partial Y}{\partial p}\right|\frac{K_1}{\rho}\,d\rho.$$

Adding to dS_1 the value $-dp$ and dividing by $d\rho$, we find

$$\frac{\partial\sigma_1^e}{\partial\rho} = \frac{-dp + dS_1^e}{d\rho} = \frac{K_1 + \frac{4}{3}\mu_1}{\rho} = a_e^2, \quad \frac{\partial\sigma_1^p}{\partial\rho} = \frac{-dp + dS_1^p}{d\rho} = \frac{K_1}{\rho}\left(1 + \frac{2}{3}\left|\frac{\partial Y}{\partial p}\right|\right) = a_p^2$$

(a_e, a_p are elastic and plastic speeds of sound). In the vicinity of the point $p_z - 0$ we have $|\partial Y/\partial p| = 3/2$, and for iron $\mu_1/K_1 \simeq 0.5$, from which $a_e^2 = 1.6K_1/\rho$, $a_p^2 = 2K_1/\rho$; as a result, the inequality $dS_1^e < dS_1^p$ holds. From the given inequality it follows that rarefaction from the point p_z occurs elastically along the dot-and-dash line in Fig. 5. At the point $p_z - 0$ the velocity of the rarefaction wave $a_+ = \sqrt{(K_1 + (4/3)\mu_1)/\rho}$ satisfies the inequality $a_+ > a_-$; therefore when intersecting the point p_z the speed of sound increases abruptly from a_- to a_+ in the rarefaction wave. As mentioned in [15], the mass velocity v remains a continuous function ($I^- = \text{const}$, $v = -\int a\,d\rho/\rho + \text{const}$); as a result, the sharp increase of a leads to an intersection of characteristics in the rarefaction wave and an RSW appears (Fig. 6, where the heavy line is for the RSW, the point z denotes the moment of its appearance, and lines 1–4 are for the RSW characteristics).

Figure 7 shows the dependence of σ on the specific volume V, where $\sigma = -\sigma_1$, $\sigma_1 = S_1 - p$, and the break at point A corresponds to the jump of the speed of sound $[a]$. The broken line denotes the Rayleigh line responsible for the RSW. As follows from Fig. 7, the flow is supersonic ahead of the RSW (in the system of the RSW front) and subsonic behind the RSW; so the conditions of evolutionary stability of the RSW are satisfied [16]. Further growth of the RSW jump is similar to that in [15]. On the one hand, RSW overtakes the characteristics 1; on the other hand, the characteristics 4 overtake the RSW. As a result, the RSW shown in Fig. 7 by the segment BC grows until point C reaches point E and point B reaches point D. The line tangential to the curve $\sigma(V)$ coincides with DE at point D, and the speed of sound $a_D = V_D\sqrt{-(\partial\sigma/\partial V)_D}$ equals the propagation velocity of the RSW through the material behind it, $v_D = V_D\sqrt{(\sigma_E - \sigma_D)/(V_D - V_E)}$. The appropriate RSW in the plane S_1, p are shown by the broken lines BC and DE (see Fig. 5).

In the present example the final state (point B in Fig. 5) is first in the elastic region, then at point F it passes to the plastic region and moves along the curve $Y(p)$ to point D. The point F' (see Fig. 5) can be to the

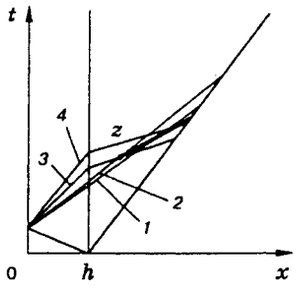

Fig. 6

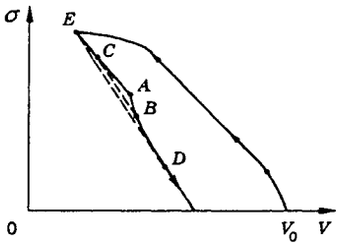

Рис. 7

left of D (the contact point of the curve $Y(p)$ and the Rayleigh line ED). If the final state in the rarefaction wave X is in the elasticity region at a straight line AF', then the stress in the RSW changes abruptly from the initial state E to the final state X. If the final state X is in the plasticity region at the curve $Y(p)$, then the RSW decays into an RSW, a constant-stress plateau, and a rarefaction wave. The RSW amplitude from point A will grow until the final state reaches point F'. At point F' the modulus of the tangent of the slope of the Rayleigh line $(3/2)|\Delta S_1/\Delta p|$ is greater than $|\partial Y/\partial p|$, so the RSW velocity is greater than that of a plastic rarefaction wave c_p. As a result, the stress in the RSW decreases abruptly from point E to point F'. Behind this jump there is a constant-stress plateau, which is adjoined by the rarefaction wave propagating with the velocity

$$\frac{dx}{dt} = v + a_x, \qquad a_x = \sqrt{\frac{K_1}{\rho}\left(1 + \frac{2}{3}\left|\frac{\partial Y}{\partial p}\right|_{F'}\right)}.$$

The final state in the rarefaction wave corresponds to the point X.

From a mathematical viewpoint the RSW is a first-order discontinuity, and the relation must be found at this discontinuity. For this purpose we rewrite Eq. (1) in a divergent form

$$\frac{\partial \rho}{\partial t} + \frac{\partial}{\partial x}(\rho v) = 0, \quad \frac{\partial}{\partial t}(\rho v) + \frac{\partial}{\partial x}(\rho v^2 - \sigma_1) = 0,$$
$$\frac{\partial}{\partial t}(\rho(\mathcal{E} + v^2/2)) + \frac{\partial}{\partial x}(\rho v(\mathcal{E} + v^2/2 - \sigma_1/\rho)) = 0.$$

Passing on to the RSW system, assuming stationary flow, we obtain after integration

$$[\rho u] = 0, \quad [\rho u^2 - \sigma_1] = 0, \quad [H + u^2/2] = 0, \quad H = \mathcal{E} - \sigma_1/\rho, \quad [\varphi] = \varphi_+ - \varphi_-, \quad H = H(\sigma_1, S),$$

where H is enthalpy; $u = v - D$; D is RSW velocity; S is entropy. These equations coincide with the relations on a shock wave in gasdynamics, if one makes the substitution $\sigma_1 \to -p$ in them. Therefore, to determine the entropy jump $[S]$ in a weak RSW one can use the appropriate formula from gasdynamics [16]. After replacing p by σ we have

$$S_+ - S_- = \frac{1}{12T_-}\left(\frac{\partial^2 V}{\partial \sigma^2}\right)(\sigma_+ - \sigma_-)^3 \tag{5}$$

($\overset{\circ}{V} = 1/\rho$). The dependence $\sigma = \sigma(V, S)$ is given in Fig. 7, whence it follows that the inverse function $V = V(\sigma, S)$ is two-valued. At fixed σ one value of V lies on the shock adiabat of loading and the other on the rarefaction adiabat. In the rarefaction wave all states lie at the rarefaction adiabat; therefore, selecting the latter, we find that $V = V(\sigma)$ is a single-valued function here. It is evident from Fig. 7 that at point A the function $V = V(\sigma)$ has a break. That is why to apply Eq. (5), one should first "disperse" $\sigma = \sigma(V)$ in

the vicinity of point A. As a result we obtain

$$\frac{\partial^2\sigma}{\partial V^2} \approx \frac{\left(\frac{\partial\sigma}{\partial V}\right)_+ - \left(\frac{\partial\sigma}{\partial V}\right)_-}{V_+ - V_-}.$$

Hence it follows that at point A ($\sigma = -p_z$) the derivative $\partial^2 V/\partial\sigma^2 < 0$, and at $\sigma_+ < \sigma_-$ the inequality $S_+ > S_-$ will hold, i.e., the entropy in the RSW increases. [The sign of the derivative $\partial^2 V/\partial\sigma^2$ follows from the relation $\partial^2 V/\partial\sigma^2 = -(1/(\partial\sigma/\partial V)^3)(\partial^2\sigma/\partial V^2)$ and the inequalities $\partial\sigma/\partial V < 0$, $\partial^2\sigma/\partial V^2 < 0$.] The RSW at phase transitions were predicted theoretically in [15] and found experimentally in metals [17] and gas-liquid media near the "liquid–vapor" critical point [18]. It should be noted that the RSW in iron [17] is connected with a polymorphic phase transition which takes place at a pressure of the order of 150 GPa which is greater than the maximum pressure considered in this work by more than a factor of 3. The generation of RSW in [17, 18] is concerned with the existence of points where $\partial^2 V/\partial p^2 < 0$, which in turn occur during phase transitions. In this case the appearance of a point with $\partial^2 V/\partial\sigma^2 < 0$ is due to the strength properties of the porous body.

Under the effect of pressure p the microstresses σ'_{ij} with nonzero deviator S'_{ij} are concentrated in the vicinity of the pores. If the pressure is $|p| > |p_0|$, then there appears a plastic zone which grows with the increase of pressure and when $|p| > |p_z|$ occupies the whole volume. As a result, the yield strength Y and the mean stress deviator S_{ij} become equal to zero. In this case the mechanical behavior of the porous material is similar to that of a liquid ($\sigma_{ij} = -p\delta_{ij}$) and the speed of sound is $a = \sqrt{K/\rho}$. As the pressure decreases below $|p_z|$, elastic zones appear in the porous body so that the deviator of mean stresses S_{ij} becomes nonzero and $\sigma_{ij} = -p\delta_{ij} + S_{ij}$. As a result, the speed of sound increases abruptly to $a = \sqrt{(K + (4/3)\mu)/\rho}$ and the RSW generates.

The RSW generation in a porous body occurs only in the case of incomplete filling of the pores in a SW and is related to the dependence of the yield strength Y of a porous body on the pressure p. If the pores are completely filled in a SW ($m_1 = 0$), no RSW is generated since $Y = Y_s = \text{const}$. The calculations carried out with $v_p = 0.642$ mm/μsec and $m_1^0 = 10^{-2}$ have shown that unloading occurs in this case in the same way as in a continuous elastoplastic material.

REFERENCES

1. T. D. Shermergor, *Theory of Elasticity of Microinhomogeneous Media* [in Russian], Nauka, Moscow (1977).
2. Z. Khashin, "Elastic moduli of nonhomogeneous materials," in: *Applied Mechanics* [Russian translation], **29**, No. 1 (1962).
3. J. Eshlby, *Continuum Theory of Dislocations* [Russian translation], Izd. Inostr. Lit., Moscow (1963).
4. R. Hill, "Elastic properties of composite media: some theoretical principles," in: *Mechanics* [Russian translation] (1964).
5. A. L. Garson, "Continuum theory of viscous fracture due to pore formation and growth. Part 1. Yield criterion and the laws of flow for a porous plastic medium," *Trans. ASME, J. Basic Eng.*, No. 1, 1–16 (1975).
6. V. Tvergard, "Numerical study of localization in a void-sheet," *Int. J. Solids Struct.*, **25**, No. 10, 1143 (1989).
7. J. N. Jonson and F. L. Adessio, "Tensile plasticity and ductile fracture," *J. Appl. Phys.*, **64**, 6699–6712 (1988).
8. M. M. Carrol and A. C. Holt, "Static and dynamic pore collapse relations for ductile porous materials," *J. Appl. Phys.*, **43**, 1626–1635 (1972).
9. S. P. Kiselev, G. A. Ruev, A. P. Ruev, et al., *Shock-Wave Processes in Two-Component and Two-Phase Media* [in Russian], Nauka, Novosibirsk (1992).

10. S. P. Kiselev and V. M. Fomin, "A model of a porous material with allowance for a plastic zone appearing near the pore," *Prikl. Mekh. Tekh. Fiz.* , **34**, No. 6, 125–133 (1993).
11. S. P. Kiselev, "Numerical modeling of propagation of elastoplastic waves in a porous material," Preprint No. 6-94, Inst. Theor. and Appl. Mech., Sib. Div., Russian Acad. of Sciences (1994).
12. V. N. Aptukov, P. K. Nikolaev, and V. I. Romanchenko, "Structure of shock waves in porous iron at low pressures," *Prikl. Mekh. Tekh. Fiz.*, No. 4, 92–98 (1988).
13. M. L. Wilkins, "Calculation of elastoplastic flows," in: *Computational Methods in Hydrodynamics* [Russian translation], Mir, Moscow (1967), pp. 212–263.
14. S. P. Kiselev, "Dynamic plasticity peak at high-rate failure of metallic shells," *Prikl. Mekh. Tekh. Fiz.*, No. 2, 122–127 (1991).
15. Ya. B. Zel'dovich and Yu. P. Raizer, *Physics of Shock Waves and High-Temperature Hydrodynamic Phenomena* [in Russian], Nauka, Moscow (1966).
16. L. D. Landau and E. M. Lifshits, *Hydrodynamics* [in Russian], Nauka, Moscow (1986).
17. A. G. Ivanov, S. A. Novikov, and Yu. I. Tarasov, "Spalling phenomena in iron and steel due to the interaction of rarefaction shock waves," *Fiz. Tverd. Tela*, No. 4, 87 (1962).
18. S. S. Kutateladze, Al. A. Borisov, A. A. Borisov, and V. E. Nakoryakov, "Experimental detection of a rarefaction shock wave near the "liquid–vapor" critical point," *Dokl. Akad. Nauk SSSR*, **252**, No. 3, 595–598 (1980).